ACTA IMEKO
ISSN: 2221-870X
Month year, Volume A, Number B, XX - YY

Model Parameter Identification from Measurement Data for Dynamic Torque Calibration – Results and Validation

Leonard Klaus

Physikalisch-Technische Bundesanstalt, Bundesallee 100, 38116 Braunschweig, Germany

ABSTRACT
The dynamic calibration of torque transducers requires the modelling of the measuring device and of the transducer under test. The transducer's dynamic properties are described by means of model parameters, which are going to be identified from measurement data. To be able to do so, two transfer functions are calculated. In this paper, the transfer functions and the procedure for the model parameter identification are presented. Results of a parameter identification of a torque transducer are also given, and the validity of the identified parameters is analysed.

Section: RESEARCH PAPER

Keywords: Mechanical modelling, model-based calibration, linear and time invariant system

Citation: Thomas Bruns, Dirk Röske, Paul P.L. Regtien, Francisco Alegria, Template for an IMEKO event paper, Acta IMEKO, vol. A, no. B, article N, month year, identifier: IMEKO-ACTA-0A (year)-0B-0N

Section Editor: name, affiliation

Received month day, year; **In final form** month day, year; **Published** month year

Funding: This work was part of the Joint Research Project IND09 *Traceable Dynamic Measurement of Mechanical Quantities* of the European Metrology Research Programme (EMRP). The EMRP is jointly funded by the EMRP participating countries within EURAMET and the European Union.

Corresponding author: Leonard Klaus, e-mail: leonard.klaus@ptb.de

1. INTRODUCTION

Several applications with dynamic torque excitation require traceable measurement. At present, only standards and procedures for the static calibration of torque transducers exist. Static calibration is an insufficient base for an analysis of dynamic measurements in terms of measurement uncertainties and influences from dynamic signal components. To be able to describe the dynamic influences of a torque transducer on a measurement set-up and vice versa, a corresponding calibration is mandatory [1]. Therefore, a measuring device and procedures for a dynamic characterisation of torque transducers were developed in the context of a joint European research project [2].

This paper is a substantially extended version of a contribution to the XXI IMEKO World Congress 2015 [3] and includes additional measurement results and analyses for the validation of the correctness of the identified parameters.

2. DYNAMIC TORQUE MEASURING DEVICE

The measurement principle of the dynamic torque measuring device (depicted in Figure 1) is based on Newton's second law. The product of a known static mass moment of inertia J of a body and a measured time-dependent angular acceleration $\ddot{\varphi}(t)$ equals the time-dependent torque

$$M(t) = J \cdot \ddot{\varphi}(t) \quad . \tag{1}$$

The measuring device consists of a rotatable vertical shaft assembly, on which all essential components are arranged in series.

At the bottom, a rotational exciter generates a forced excitation by means of sinusoidal oscillations. The torque transducer under test (device under test, DUT) is arranged on top of the exciter between two coupling elements. These couplings are designed to be both torsionally stiff and compliant for parasitic bending moments and axial loads simultaneously. At the top, the arrangement of the DUT and the couplings is followed by an angular grating disk for the angular acceleration measurement and an air bearing to prevent axial loads acting on the components of the drive shaft.

The angle position at the top (φ_{M}) is measured by means of a laser Doppler vibrometer and the radial grating disk. The angular acceleration at the bottom ($\ddot{\varphi}_{\mathrm{E}}$) is measured by an angular accelerometer embedded in the rotor of the rotational exciter.

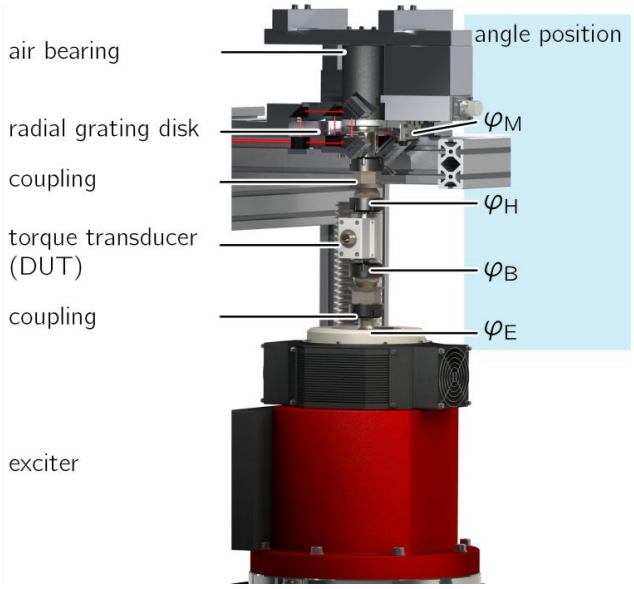

Figure 1. Dynamic torque measuring device with the different components arranged vertically on top of the exciter.

3. MODELLING

The dynamic behaviour of the transducer under test is described by a linear time-invariant (LTI) model. It is based on the mechanical design of typical strain gauge torque transducers. The model consists of two rigid mass moment of inertia elements (MMOI) which are connected by a massless torsional spring and damper in parallel. A sole modelling of the transducer under test is not sufficient, because of the fact that the dynamic behaviour of torque transducers can be influenced by the coupled components. Torque transducers are always coupled to their mechanical environment at both sides which causes a bidirectional influence on the dynamic behaviour of the torque transducer and the coupled mechanical components (which are always arranged in some type of drive assembly).

To be able to identify the model parameters of the DUT, the modelling was expanded from the model of the transducer to a model of the whole measuring device, which is the mechanical environment in the case of the calibration. The model again consists of mass moment of inertia elements, torsional springs and dampers, assuming the LTI behaviour of the measuring device. It is based on the mechanical design of the components of the drive shaft. The representation of the model components and the corresponding components of the measuring device are given in Figure 2.

This model can be described by a set of inhomogeneous ordinary differential equations (ODEs). With the mass moment of inertia matrix $\boldsymbol{J}$, the torsional stiffness matrix $\boldsymbol{K}$ and the damping matrix $\boldsymbol{D}$ there follows

$$\boldsymbol{J} \cdot \ddot{\boldsymbol{\varphi}} + \boldsymbol{D} \cdot \dot{\boldsymbol{\varphi}} + \boldsymbol{K} \cdot \boldsymbol{\varphi} = \boldsymbol{M} \ . \tag{2}$$

The angle vector $\boldsymbol{\varphi}$ describes the angle excitations at different positions in the model; its derivatives $\dot{\boldsymbol{\varphi}}$ and $\ddot{\boldsymbol{\varphi}}$ represent the angular velocity and angular acceleration, respectively. The load vector $\boldsymbol{M}$ describes the excitation of the rotational exciter.

Based on this equation system, the model parameter identification will be carried out.

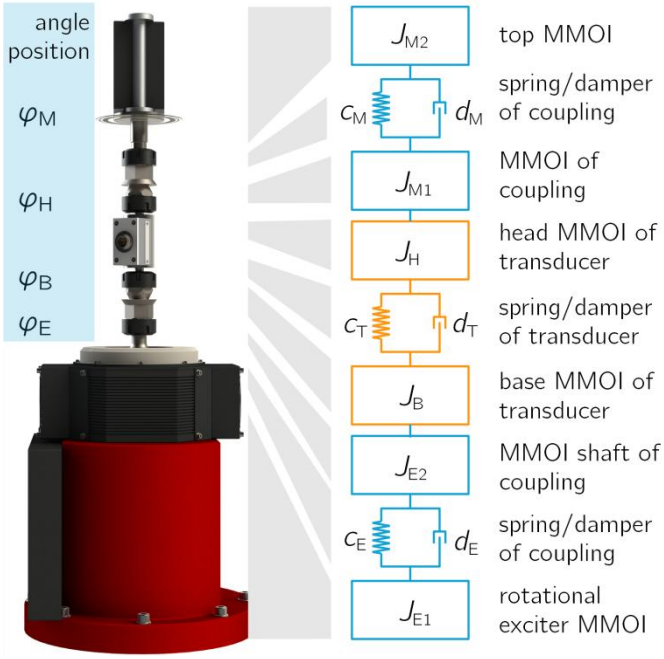

Figure 2. Dynamic torque measuring device (left) and corresponding model representation (right) of the measuring device (blue) and the DUT (orange).

The excitation signals chosen are monofrequent sinusoids. With these harmonic waveforms, not all necessary angle position, angular velocity and angular acceleration data has to be derived independently or by numerical differentiation / integration but can be calculated as follows

$$\begin{aligned} \varphi(t) &= \hat{\varphi} \cdot \mathrm{e}^{\mathrm{i}\omega t} \ , \\ \dot{\varphi}(t) &= \mathrm{i}\omega \ \hat{\varphi} \cdot \mathrm{e}^{\mathrm{i}\omega t} = \ \mathrm{i}\omega \ \varphi(t), \\ \ddot{\varphi}(t) &= -\omega^2 \ \hat{\varphi} \cdot \mathrm{e}^{\mathrm{i}\omega t} = \ -\omega^2 \ \varphi(t), \end{aligned} \tag{3}$$

where $\mathrm{i} = \sqrt{-1}$ denotes the imaginary number.

Measurements are not possible at all angle positions given in (2) and depicted in Figure 2. To gather the information necessary for parameter identification, the output signal of the transducer U_{DUT} is used as an indicator for the difference in the torsion angle above and below the transducer. This assumption is valid, because it is assumed that the output signal of the transducer is proportional to its torsion $\Delta\varphi_{\mathrm{HB}} = \varphi_{\mathrm{H}} - \varphi_{\mathrm{B}}$ giving

$$U_{\mathrm{DUT}}(t) \propto \Delta\varphi_{\mathrm{HB}}(t) \, . \tag{4}$$

During calibration, three measurement signals are acquired simultaneously. The signals will be processed to determine the magnitude and phase of each harmonic and monofrequent signal by means of a sine fit.

4. KNOWN AND UNKNOWN MODEL PARAMETERS

A prerequisite for the model parameter identification of the unknown parameters of the transducer under test is a sufficiently low number of unknown model parameters of the system. To this end, the necessary parameters of the measuring device were determined in advance. The properties of the measuring device will not change for different transducers, and therefore needed to be determined only once. Three auxiliary measurement set-ups for the measurement of the mass moment of inertia, torsional stiffness and rotational damping were developed [4][5] and the corresponding properties of the measuring device's components were determined. The only

model parameters to remain unknown prior to the model parameter identification are the parameters of the transducer under test.

5. TRANSFER FUNCTIONS

The three available signals acquired during calibration measurements are used to calculate two complex transfer functions of the system in the frequency domain. One transfer function $H_{\mathrm{top}}(\mathrm{i}\omega)$ describes the dynamics of the top part of the measuring device giving

$$H_{\mathrm{top}}(\mathrm{i}\omega) = \frac{\rho \cdot \Delta\varphi_{\mathrm{HB}}(i\omega)}{\ddot{\varphi}_{\mathrm{M}}(i\omega)} \tag{5}$$

with the (still unknown) proportionality factor ρ linking the voltage output of the transducer to its torsion (cf. (4)).

The same applies to the bottom part of the measuring device giving the transfer function

$$H_{\mathrm{bott}}(\mathrm{i}\omega) = \frac{\rho \cdot \Delta\varphi_{\mathrm{HB}}(i\omega)}{\ddot{\varphi}_{\mathrm{E}}(i\omega)} \ . \tag{6}$$

The two transfer functions are illustrated in Figure 3. The underlying ODE system gives the corresponding equations for both transfer functions. The derivation of these relations is more thoroughly described in [5].

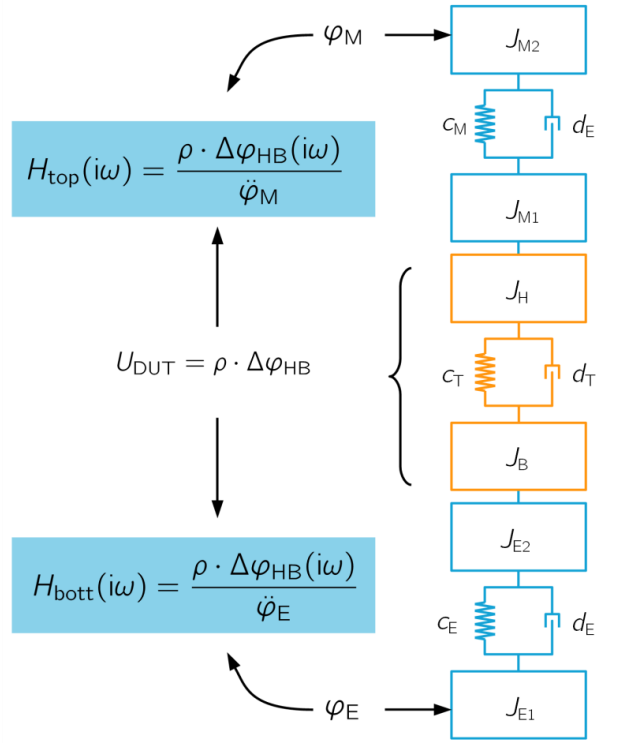

Figure 3. The two calculated transfer functions based on the acquired measurands.

6. MODEL PARAMETER ESTIMATION

The model parameter identification is carried out based on the two transfer functions. Each acquired measurement data point is a sample with random deviations. For the identification of the parameters of the DUT with evaluated uncertainties and known deviations, the occurrence of these statistical influences has to be taken into account.

A transfer function $H(\mathrm{i}\omega)$ describes the relation between input $X(\mathrm{i}\omega)$ and output $Y(\mathrm{i}\omega)$ as follows

$$Y(\mathrm{i}\omega) = H(\mathrm{i}\omega) \cdot X(\mathrm{i}\omega) \ . \tag{7}$$

For the derived frequency responses from the measurement data, a best set of model parameters needs to be chosen to fulfil this relation as well as possible. However, due to the measurement uncertainty deviations, which will always occur, an exact measurement of $X(\mathrm{i}\omega)$, $Y(\mathrm{i}\omega)$ will not be possible. The measured data will always be disturbed randomly due to the measurement uncertainty. The vectors of measurement data $X_{\mathrm{M}}(\mathrm{i}\omega)$, $Y_{\mathrm{M}}(\mathrm{i}\omega)$ are therefore multivariate random vectors with estimated state of knowledge probability density functions (PDF). Figure 4 depicts the relation of the measured input and output quantities and the model transfer function.

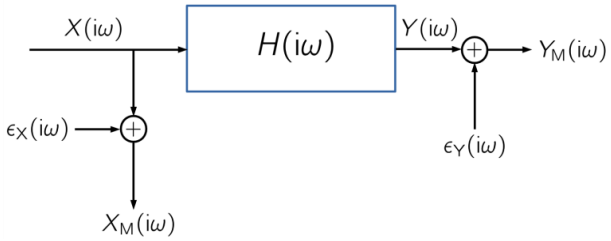

Figure 4. Schematic illustration of a transfer function and its relation to input and output.

The more information is taken into account for the model parameter estimation, the more reliable the outcome can be. Based on the chosen estimator, knowledge about the input quantities, the output quantities, and about the parameters to be identified prior to the estimation (so-called *a priori* knowledge) can be considered.

Three typical estimators are compared regarding their demand of knowledge of the different quantities in Table 1. A '+' indicates necessary information about the distribution of a quantity; a '−' indicates that it is not necessary to know the distribution.

Table 1. Requirements of different estimators.

knowledge about → estimator ↓	distribution of input quantities	distribution of the (unknown) parameters
Bayes' estimator	+	+
maximum likelihood estimator	+	−
least squares estimator	−	−

The classical frequentist approach to a model parameter estimation takes no uncertainty contributions in terms of PDFs of input quantities into account. Therefore, the estimated set of parameters consists of the estimated values, but not of information about their distribution. The least squares (LS) estimator and the maximum likelihood estimator are frequentist estimation approaches.

The *least squares estimator* minimises the squared sum of residuals of a complex model function $\boldsymbol{G}$ and of the measurement data $\boldsymbol{X}_{\mathrm{M}}(\mathrm{i}\omega)$, $\boldsymbol{Y}_{\mathrm{M}}(\mathrm{i}\omega)$ for n data points giving

$$\widehat{\boldsymbol{\theta}}_2 = \arg\min_{\widehat{\boldsymbol{\theta}}_2} \sum_{i=1}^{n} \left(\left(\boldsymbol{X}_{\mathrm{M},i}(\mathrm{i}\omega), \boldsymbol{Y}_{\mathrm{M},i}(\mathrm{i}\omega) \right) - \boldsymbol{G}(\mathrm{i}\omega, \boldsymbol{\theta}_1, \widehat{\boldsymbol{\theta}}_2) \right)^2 . \tag{8}$$

In the case of the model parameter estimation of torque transducers, the model function consists of a vector of

parameters of the measuring device $\boldsymbol{\theta}_1$, which is known, and the vector of unknown parameters of the transducer under test $\widehat{\boldsymbol{\theta}}_2$, which is estimated. No weighting of the different values is applied with this estimator.

The maximum likelihood function ℓ for a vector of samples $\boldsymbol{x} = [x_1, x_2, \dots, x_n]^T$ with the sample's PDF $p(x_i, \boldsymbol{\theta})$ for the estimation of the parameters $\boldsymbol{\theta}$ is the joint PDF of all samples giving

$$\ell(x, \theta) = p(\, x \mid \theta\,) = \prod_{i=1}^{n} p(x, \theta)\ . \tag{9}$$

Assuming normally distributed input quantities for the dynamic torque application described; the maximum likelihood function leads to

$$\ell(i\omega, \boldsymbol{\theta}_1, \boldsymbol{\theta}_2, \boldsymbol{X}_\mathrm{M}, \boldsymbol{Y}_\mathrm{M}) \propto \prod_{i=1}^{n} \mathrm{e}^{-\frac{\left(\left(X_{\mathrm{M},i}(\mathrm{i}\omega), Y_{\mathrm{M},i}(\mathrm{i}\omega)\right) - \boldsymbol{G}(\mathrm{i}\omega, \boldsymbol{\theta}_1, \boldsymbol{\theta}_2)\right)^2}{2u_i^2}}. \tag{10}$$

with the measurement data $X_{\mathrm{M},i}$, $Y_{\mathrm{M},i}$, the corresponding measurement uncertainties u_i, and the model function $\boldsymbol{G}$. The likelihood function is maximised for the parameter estimation. The estimated parameters $\widehat{\boldsymbol{\theta}}_2$ are given by

$$\widehat{\boldsymbol{\theta}}_2 = \arg\max_{\hat{\boldsymbol{\theta}}_2} \ell(i\omega, \boldsymbol{\theta}_1, \boldsymbol{\theta}_2, \boldsymbol{X}_\mathrm{M}, \boldsymbol{Y}_\mathrm{M})\ . \tag{11}$$

For independent and normally distributed input quantities, the maximum likelihood estimator can be reduced to a weighted least squares (WLS) estimator [6]. Then, the parameter estimation can be carried out with the standard uncertainties of the measurement data u_i as follows

$$\widehat{\boldsymbol{\theta}}_2 = \arg\min_{\hat{\boldsymbol{\theta}}_2} \sum_{i=1}^{n} \frac{\left(\left(\boldsymbol{X}_{\mathrm{M},i}(\mathrm{i}\omega), \boldsymbol{Y}_{\mathrm{M},i}(\mathrm{i}\omega)\right) - \boldsymbol{G}(\mathrm{i}\omega, \boldsymbol{\theta}_1, \boldsymbol{\theta}_2)\right)^2}{2u_i^2} \tag{12}$$

applying one of the widely available WLS estimators. For the given application, the induced errors are based on the different measurement quantities and need to be quantified by a measurement uncertainty evaluation. Based on this analysis, a correct weighting of the input measurement channels can be carried out.

The uncertainties of the estimated parameters cannot be calculated directly for the frequentist approaches. The calculation of lower uncertainty limits or of confidence intervals is not applicable for the dynamic torque calibration, because the influences of the uncertainties of the parameters of the measurement ($p(\boldsymbol{\theta}_1)$) are invisible for the estimator.

Therefore, the uncertainty evaluation of the estimated parameters will be carried out according to the recommendations of the *Guide to the expression of uncertainty in measurement* [8] (GUM) and its Supplement 1 [9], respectively. A Monte Carlo simulation with all input PDFs will be carried out to evaluate the uncertainty of the estimated parameters.

Differently from the frequentist approach, a parameter estimation based on Bayes' statistics assumes all parameters to be uncertain. Based on Bayes' theorem, the *a posteriori* PDF follows from the *a priori* PDF, the evidence's PDF and the likelihood (cf.(9)) giving

$$p(\text{a posteriori}) = \frac{\text{likelihood} \cdot p(\text{a priori})}{p(\text{evidence})} \tag{13}$$

For the parameter estimation of torque transducers, the latter equation leads to

$$p\left(\, \theta_1, \hat{\theta}_2 \mid \boldsymbol{X}_M, \boldsymbol{Y}_M \,\right) = \frac{\ell(i\omega, \boldsymbol{\theta}_1, \boldsymbol{\theta}_2, \boldsymbol{X}_\mathrm{M}, \boldsymbol{Y}_\mathrm{M})\, p_0(\boldsymbol{\theta}_1)\, p_0(\boldsymbol{\theta}_2)}{p(\boldsymbol{X}_\mathrm{M})\, p(\boldsymbol{Y}_\mathrm{M})}. \tag{14}$$

It becomes obvious that the measurement uncertainty is inherent in a parameter estimation by means of a Bayes' estimator, including uncertainty contributions of the parameters of the measuring device $p_0(\boldsymbol{\theta}_1)$, the contributions of the uncertainty of the measurement data, and contributions of prior knowledge of the parameters to be estimated $p_0(\boldsymbol{\theta}_2)$. The prior distribution of the parameters to be estimated does not need to be known exactly prior to the estimation (although this is mentioned accordingly in literature [7]); instead reasonable initial PDFs should be available.

Despite all of its advantages, the Bayes' estimator is still rarely used for parameter estimation of mechanical systems. It requires much more effort than LS approaches to be implemented, because it has to be developed individually for each application, whereas for the least-squares-based approaches, an application of the widely available LS algorithms is possible. This effort is the reason why this paper focuses on the least squares approaches in a first step. However, it is planned to develop a Bayes' estimator for the application to dynamic measurements of mechanical quantities in the future.

7. MODEL PARAMETER ESTIMATION

The parameter estimation based on the measurement data is implemented in Mathworks Matlab and in the open source scientific computing software GNU Octave. The measurement uncertainties for the three measurement channels have been estimated prior to the implementation of the maximum likelihood estimator. The measurement uncertainties are assumed to be independent and normally distributed.

Therefore, the maximum likelihood estimator is implemented as a weighted least squares estimator (cf. (12)). The weighting of the different data points of each channel is based on two conditions:

1. The measurement uncertainties of the three acquired signals are assigned to the measurement values. The combined uncertainties u_comb of the two transfer functions are calculated by means of a quadratic summation giving $u_\mathrm{comb} = \sqrt{u_1^2 + u_2^2 + \cdots + u_n^2}$ based on the uncertainty contributions of the measurement channels.
2. The uncertainty of each measurement value is taken into account by evaluating the covariance matrix of the sine approximation applied to the time series data. The variances for the approximated parameters (the diagonal elements of the covariance matrix) are normalised and inverted for the weighting.

The two resulting matrices are multiplied element by element to obtain the weighting matrix for the WLS estimator.

The equations representing the model parameters within the transfer functions are nonlinear in their parameters. Therefore, only iterative algorithms for nonlinear regression were applicable. To avoid complex numbers in the results for the model parameters, it was necessary to constrain the algorithm to real numbers in the parameter vector. To this end, one set of approximated parameters was calculated by means of the real ($\Re$) and imaginary parts ($\Im$) of the two inverse transfer

functions giving $\Re(H_{\mathrm{top}}^{-1}(\mathrm{i}\omega))$, $\Re(H_{\mathrm{bott}}^{-1}(\mathrm{i}\omega))$, $\Im(H_{\mathrm{top}}^{-1}(\mathrm{i}\omega))$, $\Im(H_{\mathrm{bott}}^{-1}(\mathrm{i}\omega))$.

8. MEASUREMENT RESULTS

The analysis of the feasibility of the parameter estimation was carried out with one HBM T5 10 N·m shaft type torque transducer (depicted in Figure 5). The chosen transducer is a passive strain gauge transducer, the bridge signals are transmitted by means of slip rings. The signal conditioning electronics, data acquisition systems, and filters have been calibrated dynamically prior to the measurements. The electrical influences of these components of the measurement chain have been compensated for [10].

Figure 5. Torque transducer HBM T5 – nominal torque 10 N·m.

For the measurement, sinusoidal excitations in a frequency range of about 10 Hz to 1 kHz can be applied. It is advantageous for the model parameter identification to include frequencies which are as high as possible, because the sensitivity to parameter changes increases with higher frequencies [6]. However, the upper frequency limit for the measurement is not only limited by the capabilities of the rotational exciter, but by the dynamic behaviour of the whole shaft assembly.

Beyond the (first) resonance frequency of the shaft assembly, the components arranged above the dominant spring element will be dynamically decoupled. The higher the excitation frequency is with respect to this resonance frequency, and the lower the damping of the system, the stronger the decoupling is.

In practice, the angular acceleration at the top of the measuring device ($\ddot{\varphi}_{\mathrm{M}}$, cf. Figure 1) will become too small and too disturbed to be reasonably measured for frequencies far beyond the resonance frequency. For the investigated transducer HBM T5 10 N·m, the upper frequency limit for the measurements was reached somewhat above 300 Hz.

The dynamic torque magnitude generated by the dynamic torque calibration device is relatively small at present and is in the range of about 0.5 N·m to 1 N·m.

Figure 6 shows the magnitude and phase responses of the complex transfer functions of the top and of the bottom of the measuring device $H_{\mathrm{top}}(\mathrm{i}\omega)$ and $H_{\mathrm{bott}}(\mathrm{i}\omega)$ for both measurement data and estimation.

The measurement results show that the deviations from the expected values of the top transfer function increase for frequencies higher than the resonance frequency of the system. This is caused by the mentioned increasing decoupling of the top part of the shaft assembly for frequencies beyond the resonance frequency.

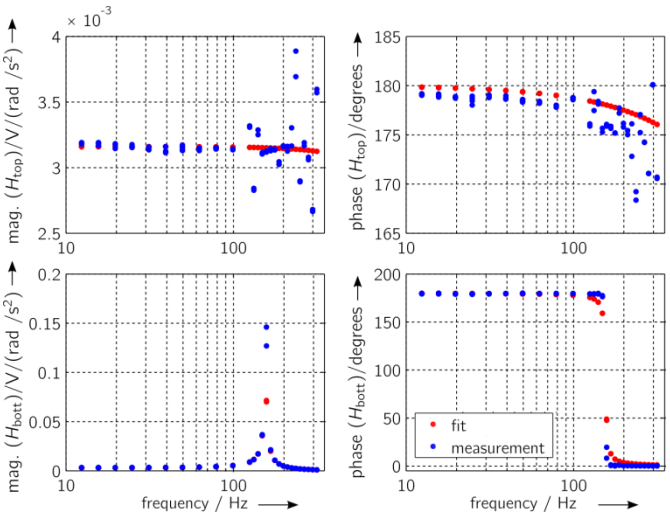

Figure 6. Measurement data of the HBM T5 transducer (blue) and fit result (red) for $H_{\mathrm{top}}(\mathrm{i}\omega)$ (top) and $H_{\mathrm{bott}}(\mathrm{i}\omega)$ (bottom) in magnitude and phase.

9. PARAMETER ESTIMATION AND VALIDATION

The results of the model parameter estimation show good agreement of the measurement data and the outcome of the regression. The identified model parameters of the investigated transducer HBM T5 are given in Table 2.

The real and imaginary parts of the two inverse transfer functions are given in Figure 7. These are the transfer functions, with which the parameter estimation was carried out.

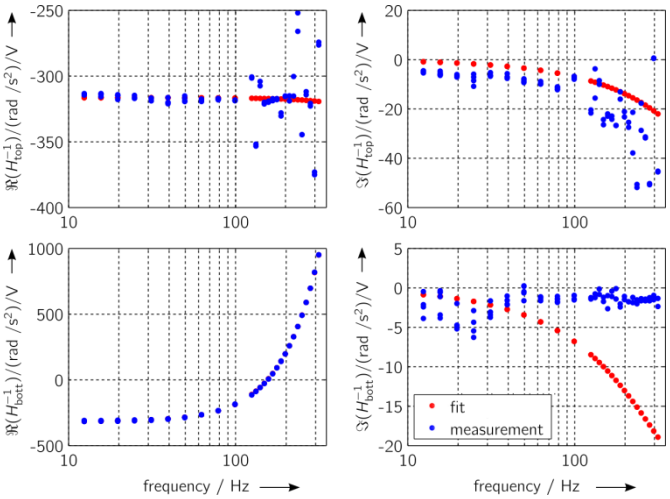

Figure 7. Measurement data of the HBM T5 transducer (blue) and fit result (red) for real ($\Re$) and imaginary ($\Im$) parts of $H_{\mathrm{top}}^{-1}(\mathrm{i}\omega)$ (top) and $H_{\mathrm{bott}}^{-1}(\mathrm{i}\omega)$ (bottom).

The real parts of the two transfer functions show very good agreement of measured values and fit, however, the imaginary parts reveal discrepancies between observed values and the regression data. To assess the correctness of the model parameters identified and to analyse the influence of the deviations in the imaginary part, a validation of the parameters was carried out based on different sources. The parameters identified describe the mechanical properties of the transducer, which can be found – to some extent – in technical data sheets. However, this information is not reliable, because neither can one ascertain how these specifications are derived, nor are any uncertainties for the given specifications available.

Table 2. Results of the parameter identification.

	J_H	c_T	d_T	J_B
measurement 1	$4 \cdot 10^{-11}\,\mathrm{kg \cdot mm^2}$	$603\,\mathrm{N \cdot m/rad}$	$3 \cdot 10^{-2}\ \mathrm{N \cdot m \cdot s/rad}$	$446\,\mathrm{kg \cdot mm^2}$
measurement 2	$8 \cdot 10^{-11}\,\mathrm{kg \cdot mm^2}$	$607\ \mathrm{N \cdot m/rad}$	$1 \cdot 10^{-2}\ \mathrm{N \cdot m \cdot s/rad}$	$272\,\mathrm{kg \cdot mm^2}$

Nevertheless, the data sheet information of the HBM T5 transducer [11] was compared with all other results.

Additionally, some parameters of the investigated transducer were determined by independent static measurements. These measurements were carried out with the auxiliary measurement set-ups already used for the determination of the mechanical properties of the measuring device [4]. While the torsional stiffness was measured without any modifications of the transducer, the friction of the slip rings and of the ball bearings made a measurement of the mass moment of inertia of the transducer's rotor by means of a pendulum set-up infeasible. Instead, a bare rotor shaft without bearings of a similar transducer (same type and same torque capacity) was used for that purpose.

It was not possible to validate the damping coefficient by independent measurements, but due to the known low damping of transducers and the large resonance rise experienced (cf. Figure 6), the influence of the damping can be assumed to be low and therefore to be less important for the dynamic behaviour of the transducer.

The results of the measurements and of the manufacturer's specifications are given in Table 3.

Table 3. Manufacturer's specifications and independent measurement results for mass moment of inertia and torsional stiffness with assigned expanded relative measurement uncertainties U_rel.

	$J = J_\mathrm{H} + J_\mathrm{B}$	$c = c_\mathrm{T}$
specifications from data sheet [11]	$41\,\mathrm{kg \cdot mm^2}$	$640\ \mathrm{N \cdot m/rad}$
measurement results	$38.6\,\mathrm{kg \cdot mm^2}$ $U_\mathrm{rel}(k=2) = 9.0\,\%$	$638.29\ \mathrm{N \cdot m/rad}$ $U_\mathrm{rel}(k=2) = 0.1\,\%$

Table 2 and Table 3 show that the data sheet specifications of the torsional stiffness agree very well with the experimental results from the auxiliary measurement, but the results from the mass moment of inertia deviate significantly.

Two issues exist for the validation of the results of the mass moment of inertia parameters of the transducer:

1. Only the overall mass moment of inertia $J = J_\mathrm{H} + J_\mathrm{B}$ can be determined by independent measurements. The top mass moment of inertia J_H was roughly estimated by means of the geometry of the rotor and with an assumed generic density of steel of $\rho \approx 7.8\,\mathrm{g/cm^3}$ giving $J_\mathrm{H} \sim 6\,\mathrm{kg \cdot mm^2}$. This number is so small that even with the set-up dedicated for the determination of mass moment of inertia, the resulting measurement uncertainty would be in the same magnitude as the measured quantity.
2. The identified mass moment of inertia parameter of the bottom part of the transducer (J_B) is significantly larger than expected. This deviation is most probably caused by the friction of the slip rings, which are arranged below the sensing element of the transducer.

To overcome these issues, an alternative validation approach was applied. The existing drive shaft assembly was modified with two different additional mass moment of inertia elements, which could be added to J_H. The design of these mass bodies was chosen in such a way that a rigid connection minimises influences due to the mounting of the adapter. The mass moment of inertia of the mass bodies was measured independently in the same way as for the rotor of the torque transducer.

One mass body is based on a modified coupling element (depicted in Figure 8); it has a mass moment of inertia of $J = 878.86\,\mathrm{kg \cdot mm^2}$ $(U_\mathrm{rel}(k=2) = 5 \cdot 10^{-4})$. Furthermore one mass body is an aluminium ring (depicted in Figure 9) with a mass moment of inertia of $= 295.64\,\mathrm{kg \cdot mm^2}$ $(U_\mathrm{rel}(k=2) = 1 \cdot 10^{-3})$.

Figure 8. Torque transducer HBM T5 (left) with the mass moment of inertia element $J \approx 900\,\mathrm{kg \cdot mm^2}$ (right).

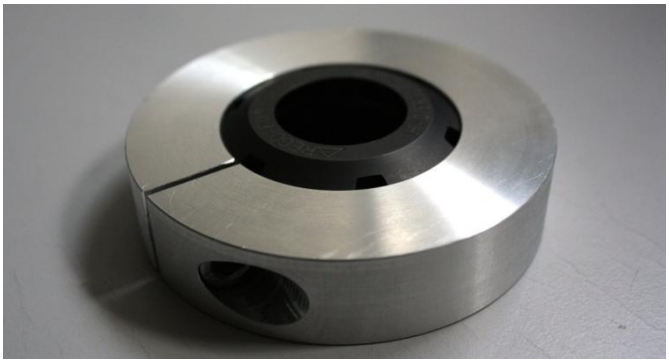

Figure 9. Moment of inertia element $J \approx 300\,\mathrm{kg \cdot mm^2}$ mounted on a clamping nut.

Both mass bodies were used for validation measurements simulating a transducer with a correspondingly larger J_H. The added mass moment of inertia in conjunction with the unchanged torsional stiffness of the torque transducer under test leads to lower resonance frequencies, and therefore to a decreased upper frequency limit for the dynamic measurements.

The measurement results for the mass moment of inertia element using the coupling element $(J \approx 900\,\mathrm{kg \cdot mm^2})$ are depicted in Figure 10, and the results for the aluminium ring $(J \approx 300\,\mathrm{kg \cdot mm^2})$ are shown in Figure 11. The resulting magnitude and phase responses of the parameters identified agree well with the corresponding measurement result. The parameters identified are given in Table 4.

Table 4. Results of the parameter identification with additional mass moment of inertia elements.

	J_H	c_T	d_T	J_B
HBM T5 with mass body $J \approx 900\ \mathrm{kg \cdot mm^2}$	$945\ \mathrm{kg \cdot mm^2}$	$637\ \mathrm{N \cdot m/rad}$	$2 \cdot 10^{-14}\ \mathrm{N \cdot m \cdot s/rad}$	$874\ \mathrm{kg \cdot mm^2}$
HBM T5 with mass body $J \approx 300\ \mathrm{kg \cdot mm^2}$	$311\ \mathrm{kg \cdot mm^2}$	$635\ \mathrm{N \cdot m/rad}$	$9 \cdot 10^{-3}\ \mathrm{N \cdot m \cdot s/rad}$	$239\ \mathrm{kg \cdot mm^2}$

For both measurements with additional mass bodies, the parameters identified agree very well with the expectations. The mass moment of inertia of the top J_H agrees excellently with the added mass moments of inertia. The torsional stiffness parameter c_T matches the independent measurements even better than with the measurements of the transducer alone. J_B is in a range similar to that of the measurements without additional mass bodies due to the influences from the friction of the slip rings. However, the reduced excitation frequency range causes higher uncertainties of the identified parameters, which will be described in a later publication.

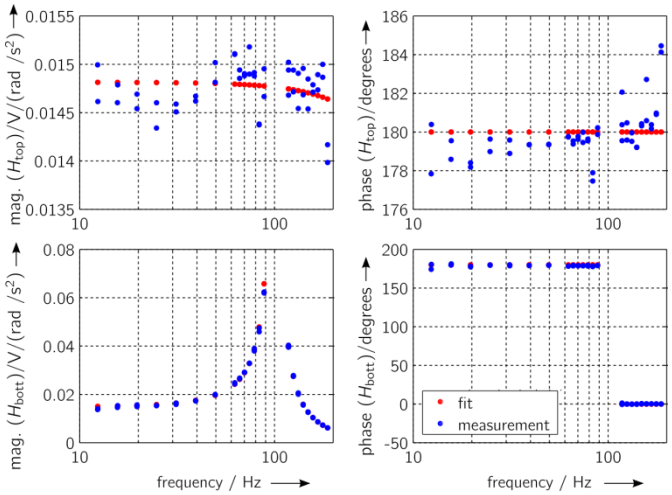

Figure 10. Measurement data of the HBM T5 transducer with additional mass moment of inertia element ($J \approx 900\ \mathrm{kg \cdot mm^2}$) (blue) and fit result (red) for $H_\mathrm{top}(\mathrm{i}\omega)$ (top) and $H_\mathrm{bott}(\mathrm{i}\omega)$ (bottom) in magnitude and phase.

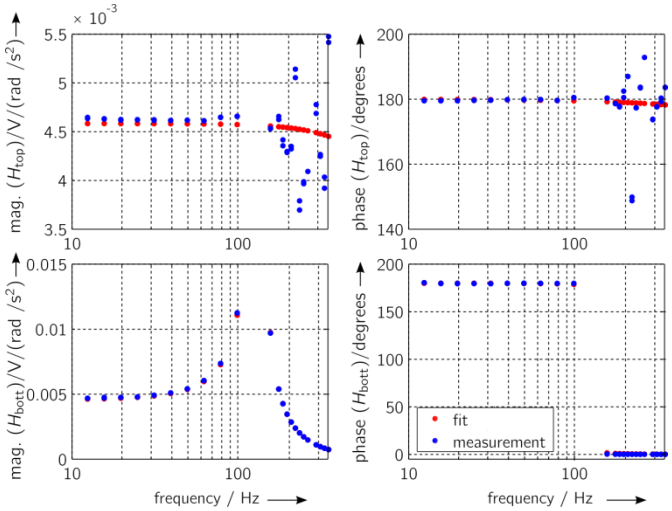

Figure 11. Measurement data of HBM T5 with additional mass moment of inertia element ($J \approx 300\ \mathrm{kg \cdot mm^2}$) (blue) and fit result (red) for $H_\mathrm{top}(\mathrm{i}\omega)$ (top) and $H_\mathrm{bott}(\mathrm{i}\omega)$ (bottom) in magnitude and phase.

10. SUMMARY AND OUTLOOK

A model-based approach enables the identification of the dynamic properties of torque transducers from measurement data. The model is linear and time-invariant and consists of known model properties of the measuring device and unknown model properties of the transducer under test. The parameter identification is carried out using the acquired measurement data which was corrected for influences from signal conditioning electronics and the data acquisition system. Three signals are acquired during the calibration measurements. Based on this data, two complex transfer functions are calculated. A nonlinear regression is carried out based on the two transfer functions to estimate a set of common parameters. These parameters describe the dynamic behaviour of the torque transducers under test.

The measurement results of the first transducer show good agreement to the model assumptions. Remaining discrepancies in the imaginary parts of the two transfer functions require further investigation.

The parameter estimation based on the measurement data gives reasonable results. A validation of identified parameters was carried out by means of independent measurements, as well as with a modified measurement set-up. The validation results agree very well with the identified parameters of the transducer and therefore confirm the results of the parameter estimation.

The estimation of the uncertainties of the measurement and of the parameter identification is beyond the scope of this paper and will be covered by a dedicated publication in future.

ACKNOWLEGDEMENT

The author would like to thank the company HBM – in particular Dr André Schäfer – for the items provided on loan (sometimes at short notice), which reduced the time needed for the validation of the parameter estimation results.

REFERENCES

[1] L. Klaus, Th. Bruns and M. Kobusch, "Dynamic Torque Calibration – Necessity and Outline of a Model-Based Approach", Proc. of 5th International Competition Best Young Metrologist of COOMET 2013, pp. 61–64, Braunschweig, Germany, June 2013, DOI: 10.7795/810.20140929.

[2] C. Bartoli et al., "Traceable Dynamic Measurement of Mechanical Quantities: Objectives and First Results of this European Project", International Journal of Metrology and Quality Engineering, vol. 3 (3), pp. 127–137, May 2013, DOI: 10.1051/ijmqe/2012020.

[3] L. Klaus, "Identification of Model Parameters of a Partially Unknown Linear Mechanical System from Measurement Data", Proc. of XXI IMEKO World Congress, Prague, Czech Republic, Sep. 2015, http://www.imeko.org/publications/wc-2015/IMEKO-WC-2015-TC3-050.pdf.

[4] L. Klaus, Th. Bruns and M. Kobusch, "Modelling of a dynamic torque calibration device and determination of model parameters", Acta IMEKO, vol. 3 (2), pp. 14–18, June 2014, http://acta.imeko.org/index.php/acta-imeko/article/viewFile/IMEKO-ACTA-03%20%282014%29-02-05/253.

[5] L. Klaus and M. Kobusch, "Experimental Method for the Non-Contact Measurement of Rotational Damping", Proc. of Joint IMEKO International TC3, TC5 and TC22 Conference 2014, Cape Town, South Africa, February 2014, http://www.imeko.org/publications/tc22-2014/IMEKO-TC3-TC22-2014-003.pdf.

[6] L. Klaus, B. Arendacká, M. Kobusch and Th. Bruns, "Dynamic Torque Calibration by Means of Model Parameter Identification", Acta IMEKO, vol. 4 (2), pp. 39–44, June 2015, http://acta.imeko.org/index.php/acta-imeko/article/view/IMEKO-ACTA-04%20%282015%29-02-07.

[7] J. Schoukens, R. Pintelon, Identification of Linear Systems – A Practical Guideline, Pergamon Press, Oxford, 1991.

[8] Bureau International des Poids et Mesures, Evaluation of measurement data — Guide to the expression of uncertainty in measurement = Évaluation des données de mesure — Guide pour l'expression de l'incertitude de mesure, 2008.

[9] Bureau International des Poids et Mesures, Evaluation of measurement data — Supplement 1 to the "Guide to the expression of uncertainty in measurement" — Propagation of distributions using a Monte Carlo method = Évaluation des données de mesure — Supplément 1 du "Guide pour l'expression de l'incertitude de mesure" — Propagation de distributions par une méthode de Monte Carlo, 2008.

[10] L. Klaus, Th. Bruns and H. Volkers, "Calibration of bridge-, charge- and voltage amplifiers for dynamic measurement applications", Metrologia, vol. 52(1), pp. 72–81, February 2015, DOI: 10.1088/0026-1394/52/1/72.

[11] Hottinger Baldwin Messtechnik GmbH, "T5 Torque Transducer Data Sheet", Version B0071-1.2, 2004.